A 1-bit Synchronization Algorithm for a Reduced Complexity Energy Detection UWB Receiver

Marco Crepaldi, Mario R. Casu, Mariagrazia Graziano and Maurizio Zamboni

Abstract— This work investigates the possibility of performing synchronization in a reduced complexity Energy Detection receiver. A new receiver scheme employing a single comparator only is defined and the related synchronization algorithm is presented. The possibility of synchronizing has been analyzed both for an idealized Dirac Delta input signal and for realistic UWB signals obtained through the TG4a channel model. The matlab simulations show that it is possible to obtain coarse synchronization using a simple maximum detection algorithm computed on collected energies for the ideal case of Dirac Delta pulses. For realistic UWB signals better synchronization performances are possible by employing a searchback algorithm. Due to the low complexity of the receiver scheme, the synchronization algorithm requires a long locking time.

Index Terms— UWB, Energy Detection, Syncronization, Low-Complexity

I. INTRODUCTION

Ultra–WideBand (UWB) is different from conventional narrowband and wideband wireless technologies. The transmission relies on short duration pulses (on the order of one nanosecond) and the signal power spectral densities are order of magnitudes lower than in other wireless systems. The combination of these two features results in the possibility of low–power consumption and in the requirement of fine time domain processing of the received pulses. The time domain computation of the received signal is fundamental both for demodulation and for determining synchronization lock–point at the receiver.

Among the possible schemes, at the receiver two approaches are commonly used: the coherent and the non–coherent ones. The first perform correlation of the incoming signal using an internally generated template. Rake–receiver structures are typically employed but unfortunately, despite their high accuracies, they are not suited for low–power applications. The second ones, aimed at the simplification of the receiver structure, do not perform any channel estimation and typically permit low–power consumptions. Among these kinds of receivers, the Energy Detection ones offer the lowest power consumption and complexity.

Coarse synchronization algorithms for Energy Detection receivers make use of simple approaches to approximately compute the pulses Time–Of–Arrival (TOA). The most common ones refer to the use of sliding integration windows to detect the time instant which corresponds to the maximum energy [1], [2], [3], [4]. The integration windows are

M. Crepaldi, M.R. Casu, M. Graziano and M. Zamboni are with the Department of Electronics, Politecnico di Torino, C.so Duca degli Abruzzi 24, I–10129, Torino, Italy (e–mail: marco.crepaldi@polito.it).

matched about to the channel spread, that is to durations on the order of tens of nanoseconds [3]. The successive fine synchronization process, aimed at refining the cluster Time–Of–Arrival estimation make use of finer sliding windows [1]. For obtaining higher performance, the synchronization can be enhanced using different approaches: In most cases popular techniques for estimating the first path time–of–arrival employ search–back algorithms [5].

This paper investigates the possibility of performing coarse synchronization in a simplified Energy Detection receiver employing a 1–bit comparator together with a search–back algorithm. This work is organised as follows: Section II presents the algorithm and defines the related mathematical models. The operation of the algorithm is explained in a simplified case in which the received pulse is a Dirac delta and finally the required modifications in the case of realistic UWB pulses are presented. Section III validates the models of the first section and presents synchronization results with idealized and realistic pulses. Finally, conclusions are drawn in section IV.

II. PROBLEM STATEMENT

The common Energy Detection receiver front–ends are inclusive of four parts (figure 1): the Low–Noise–Amplifier
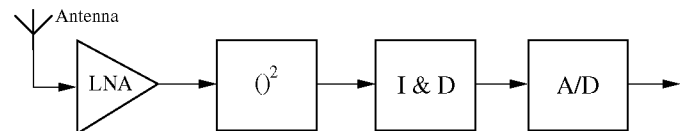

Fig. 1. Typical Energy Detection receiver

(LNA), the squaring unit ($()^2$), the Integrate–and–Dump unit (I & D) and finally the Analog–to–Digital Converter (A/D). The UWB signal is first amplified, squared and integrated for a certain duration; successively, the computed energy is converted into digital domain to allow synchronization and demodulation. A typical modulation scheme for these systems is 2–PPM (Bi–phase Pulse–Position–Modulation). It consists of the placement of the pulses in the first or in the second half of a Pulse–Repetition–Interval (PRI). The Energy Detection receiver demodulates data first by integrating each of the two halves of the PRI, and then by comparing the A/D converted energies numerically.

Typically each transmitted packet is inclusive, in the first part, of a preamble sequence containing UWB pulses modulated according to a known scheme. In this work the preamble sequence is formed by a collection of non–modulated pulses

constantly repeated according to a PRI. The preamble signal at the receiver antenna is thus expressed by,

$$r(t) = s(t) + n(t) = \sum_{i=-\infty}^{+\infty} p(t - iT_s - \tau) + n(t) \quad (1)$$

where T_s is the PRI, $p(t)$ is the UWB signal, τ is the delay between transmitter and receiver clocks and $s(t)$ is the previously defined non-modulated preamble sequence. The received signal $r(t)$ is comprehensive of Additive White Gaussian Noise (AWGN) $n(t)$.

We suppose that no A/D converters are employed at the receiver and the block which performs integration of the UWB pulses operates as a "Differential Energy Detector" (figure 2). It performs two integrations of the incoming UWB signal thanks to four control signals (schematised in figure with a single arrow) and allows to dump the obtained integrated values for successive comparisons. The time diagram on the right side of the figure summarizes the operation of the device.

The aim of this integrator is to capture the differential energy step between two successive pulses of the preamble sequence and to output a single bit which accounts for the sign of the energy difference. For doing this, the unit integrates two adjacent UWB pulses with two different integration windows delayed of t_{synch}. At the end of the process, the two obtained energies are compared and an output bit is given. The value of the bit is established according to the comparison of the obtained energies during the integration phases. The first integration of duration T_w is performed through activation of signal `int_plus` and successively dumped by signal `dump`. After the second integration started by `int_minus`, the unit makes the final comparison. Signal `reset` prepares the device for a new operation cycle. A possible implementation of the "Differential Energy Detector" is given at the bottom of the figure. It basically consists of an Operational Transconductance Amplifier (OTA) loaded with a capacitor. The operation phases presented above are carried out by the switched capacitor network connected to the OTA output.

Before discussing the operation of the algorithm in presence of real UWB signals, we simplify the problem by supposing that $p(t)$ is a Dirac delta $\delta(t)$. With this hypothesis the analytical formulation of the synchronization problem is easily derived and it is thus possible to understand its main drawbacks in presence of real UWB signals.
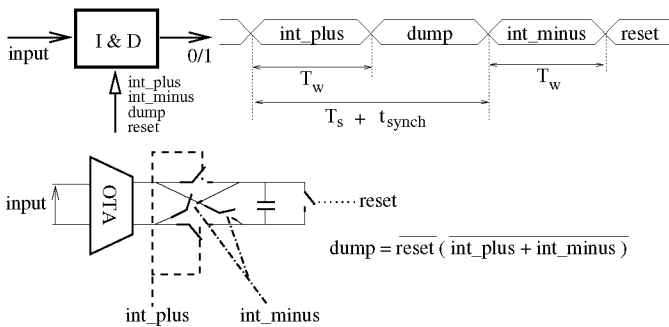

Fig. 2. Differential Energy Detector

The synchronization algorithm consists of two consecutive

parts: In the first one, called *Energy Computation*, the algorithm calculates the energy variations according to different position in time, with a sufficient resolution to determine a pre-established synchronization accuracy. In the second, the *post-processing*, it processes the computed energies to establish the position in time of the maximum energy of the received signal. We further separately analyze these two parts in the following discussion. The first subsection explains the Energy Computation process in which energies are collected. The second subsection deals with post-processing in the case $p(t) = \delta(t)$. Finally, the third subsection addresses the post-processing problem in the case of real UWB pulses.

A. Energy computation

Figure 3 shows the operation of the first phase of the algorithm at the Energy Detector input. Quantity t_{step} in figure defines the synchronization accuracy.
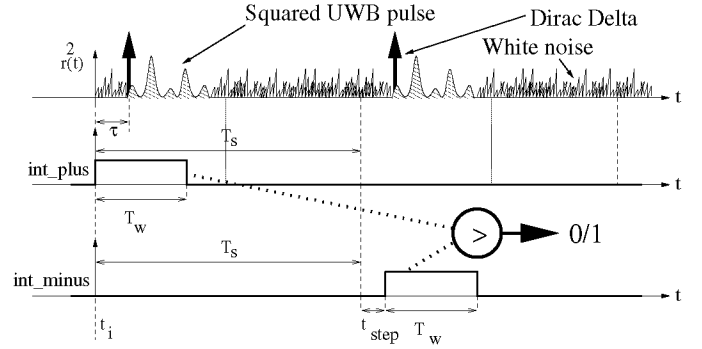

Fig. 3. Energy Computation

Quantities t_i and T_w define the integration reference time and the integration duration, respectively. We define the two computed energies as

$$I_0(i) = \int_{t_i}^{t_i + T_w} r(t)^2 dt \quad (2)$$

$$I_1(i) = \int_{t_i + t_{step} + T_s}^{t_i + t_{step} + T_s + T_w} r(t)^2 dt \quad (3)$$

where index i denotes the integration process steps and the condition $i \epsilon [0..N - 1]$ holds. In particular, $t_{i+1} = t_i + t_{step}$, where t_{step} is the synchronization accuracy. The quantity N is the number of steps performed by the algorithm and is defined as $N = \frac{T_s}{t_{step}}$. The Differential Energy Detector compares the two energies according to the sign of computation of $I_0(i) - I_1(i)$. If the result is larger than zero, its output is 0, while if it is smaller than zero its output is 1.

Thanks to the short duration of UWB pulses, supposing that T_w is large enough to let the UWB pulse be considered with zero mean, it is possible to simplify the received squared signal as follows,

$$\int r(t)^2 \simeq \int p^2(t) + \int n^2(t). \quad (4)$$

The received signal is circa a sum of two terms: The first accounts for the squared UWB input signal and the other one

is a stochastic process due to AWGN. In previous works (see [5] and references therein), it has been demonstrated that the squared and integrated AWGN can be considered as a gaussian distributed stochastic process with variance $\sigma_{ed}^2 = 4B_wT_w\sigma_n^4$ and mean $\mu_{ed} = 2B_wT_w\sigma_n^2$. The quantities B_w and σ_n are the noise equivalent bandwidth and the standard deviation of $n(t)$. These relations hold only whether $2B_wT_w > 4$. With these assumptions, it is possible to define the analog quantity computed by the Energy Detector to determine the output bit. The integrals of equations 2 and 3 can be rewritten as follows,

$$I_0(i) \simeq E_0(i) + N_0(i) \tag{5}$$

$$I_1(i) \simeq E_1(i) + N_1(i) \tag{6}$$

where $E_0(i) = \int_{t_i}^{t_i+T_w} p(t)^2 dt$ and $E_1(i) = \int_{t_i+t_{step}+T_s}^{t_i+t_{step}+T_s+T_w} p(t)^2 dt$. Quantities $N_0(i)$ and $N_1(i)$ represent the previously mentioned gaussian distributed process with variance σ_{ed}^2 and mean μ_{ed}. The output quantity processed by the comparator can be defined as $R(i) = I_0(i) - I_1(i) = (E_0(i) - E_1(i)) + (N_0(i) - N_1(i))$. This residual energy $R(i)$ is thus formed by two terms: The first is a quantity which depends on the UWB signal, while the second is a stochastic process with zero mean and twofold variance σ_N^2 with respect to σ_{ed}^2 ($\sigma_N^2 = 2\sigma_{ed}^2$), which will be compactly expressed as $E(i) + N(i)$, where $E(i) = E_0(i) - E_1(i)$ and $N(i) = N_0(i) - N_1(i)$.

After the integration of UWB pulses and noise, the Energy Detector "digitizes" the term $R(i)$ and gives a digital value $D\{R(i)\}$, where D is the "Digital Operator" which implements the comparison of its argument with a zero-threshold. During algorithm operation, the couples of integrations are spanned from 0 to $N-1$ and the obtained digital bits are grouped together in a vector. We define the DE vector as follows,

$$DE = [DE_0, DE_1, DE_2, ..., DE_i, ...DE_{N-1}] \tag{7}$$

where DE_i is defined as $D\{R(i)\}$. It is easy to show that the probability of having 0 or 1 in a specified position i, is given by the expressions

$$P(DE_i = 0) = 1 - \frac{1}{2}erfc\left(\frac{-E(i)}{\sqrt{2}\sigma_N}\right) \tag{8}$$

$$P(DE_i = 1) = \frac{1}{2}erfc\left(\frac{-E(i)}{\sqrt{2}\sigma_N}\right) \tag{9}$$

where $erfc$ is the common error function defined as $erfc(x) = \frac{2}{\sqrt{\pi}}\int_x^{+\infty} e^{-t^2} dt$. These formulas shows how the probabilities are influenced by the energy step $E(i)$ in the i-th position. In order to mitigate the effect of noise, it is possible to consider a processing gain in the energy computations. The processing consists of the repetition of the integration cycle span for PG times and then of the addition of the obtained DE vectors together. We thus define the final collection vector as,

$$ADE = [\sum_{j=1}^{PG} DE_0^j, ..., \sum_{j=1}^{PG} DE_i^j, ..., \sum_{j=1}^{PG} DE_{N-1}^j] \tag{10}$$

where DE_i^j is the i-th element at the j-th iteration. We also define the generic i-th column of vector ADE as ADE_i.

The vector contains integer values from 0 to PG. Given that the vectors DE are statistically independent, it is possible to demonstrate that, for each column i, the probabilities of detecting $[0, PG]$ are distributed as a Bernoulli density. The generic probability of computing the resulting integer value in column i, is thus expressed by

$$P(ADE_i = K) = \binom{PG}{K}\left(\frac{1}{2}erfc\left(\frac{-E(i)}{\sqrt{2}\sigma_N}\right)\right)^K \cdot \tag{11}$$
$$\left(1 - \frac{1}{2}erfc\left(\frac{-E(i)}{\sqrt{2}\sigma_N}\right)\right)^{PG-K}$$

Moreover, it is possible to relate the formula to the Signal-to-Noise Ratio (SNR) by two simple steps. The first consists of the definion of the quantity $x = \frac{E(i)}{\sqrt{2}\sigma_N}$ and the second consists of using the definition of squared noise variance and of E_b/N_0. It is thus easy to demonstrate that SNR is given by

$$\frac{E_b}{N_0} = 2x\sqrt{B_wT_w} \tag{12}$$

These calculations, as shown in the following subsection, are useful for understanding how the algorithm operates under the assumption of using a sampled Delta as UWB pulse given a certain bandwidth.

B. Post-processing for a Dirac delta UWB signal

After the first phase in which the receiver collects the samples $D\{R(i)\}$, the second phase consists of a post-processing performed on vector ADE. Considering that the aim of Energy Detection receivers is to achieve low-power consumption once implemented, this second part must be very simple and must not require complex computations. The aim here is to analyze a very simple synchronization algorithm.

In case the received UWB pulse is a Delta, supposing that no noise is present at the receiver input, vector ADE assumes a shape as shown in figure 4. The output given by the "Differential Energy Detector" is non-zero only in the case that the Delta falls within the integration domain of E_1. In the other cases, the Energy Detector gives a zero output. Hence, at very high signal to noise ratios it is possible to consider the index corresponding to the maximum of vector ADE as a reliable synchronization information. In formulas, given index
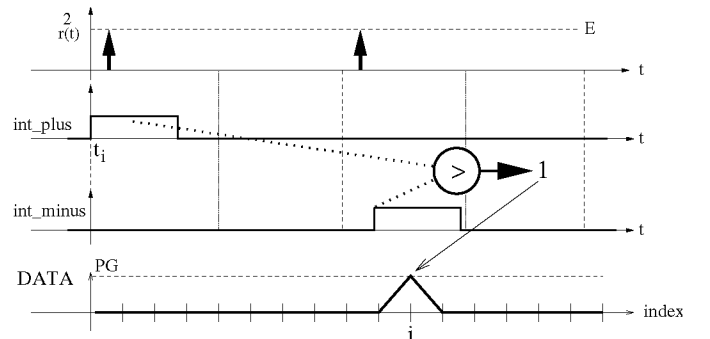

Fig. 4. Vector ADE for Dirac Delta Post-Processing, no noise

i corresponding to the maximum value in vector ADE, the decision is made by

$$i_{synch} = arg\{max_i\{ADE\}\} \qquad (13)$$

where i_{synch} represents the synchronization index and is related to the synchronization time t_{synch} by $t_{synch}=t_{step}\cdot i_{synch}$. At low SNR the situation is completely different, in particular the maximum detection algorithm misses due to the presence of noise. In other words, the position of maximum in vector ADE is not uniquely determined.

In presence of a $\delta(t)$ with energy E, the formal expression of ADE probabilities are quite simplified.[1] All the energies $E(i)$ are zero except for two positions k and j: At the LS computation time the two energy steps $E(k)$ and $E(j)$ are opposite, that is $E(k) = E$ and $E(j) = -E$. With this hypothesis, it is possible to calculate a quantity which states the relations between the algorithm parameters and the synchronization performance: the Detection Probability P_d. The general expression is given by,

$$P_d(i) = \sum_{L=1}^{PG} P(ADE_i = L) \prod_{i \neq m} P(ADE_m < L).$$

In the simplified case that, given the lock point i and supposing that the obtained value ADE_i is PG, P_d is given by

$$P_d(i) = P(ADE_i = PG \wedge ADE_{i+1} < PG \qquad (14)$$
$$\wedge ADE_{i-1} < PG \wedge ADE_{i+2} < PG...) =$$
$$= P(ADE_i = PG) \prod_{i \neq m} P(ADE_m < PG)$$

where m is a generic index from 0 to $N - 1$. Using equation 11 and equation 12, using the hypothesis $T_w/t_{synch} > 2$, the Detection Probability can be written as,

$$P_d = \frac{1}{2^{PG}} erfc^{PG}(-x) \cdot \qquad (15)$$
$$\cdot \left(1 - \frac{1}{2^{PG}} erfc^{PG}(x)\right) \left(1 - \frac{1}{2^{PG}}\right)^{N-2}.$$

This expression represents the real "Detection Probability" only for high Signal-to-Noise Ratios because it is assumed that ADE_i reaches the value of PG after PG iterations. At high processing gains on the order of 10 and for a sufficiently high energy E, the Detection Probability is maximised as will be shown further. Whether a high x is chosen, the quantity P_d tends to $(1 - \frac{1}{2^{PG}})^{N-2}$. This result suggests that the performance of the synchronization algorithm depends on the number of steps employed in the Energy Computation. Worse performances are expected in case a short synchronization step t_{synch} is employed.

This result, verified with simulations in the next section, suggests that below a certain SNR, the Detection Probability reaches a maximum value.

---

[1] This is valid only for PG sufficiently large: Whether $s(t) = \delta(t)$ the expression $\int_D \delta(t)n(t)dt \neq 0$ holds, and in the DE vector this effect is mitigated by processing gain PG, since $\sum_n^{PG} \int_{D_n} \delta(t)n(t)dt \to 0$ as $PG \to +\infty$, where D_n is the integration domain.

C. Post-processing for a realistic UWB pulse

Due to the short pulse duration, the UWB channel is rich of multipath components. The received signal is completely different from the typical sub-nanosecond transmitted pulses and the hypothesis of receiving a Dirac delta is never true. An absolute figure of the energy variations of the received signal cannot be determined because signal has a statistical nature. Referring to the analysis of previous subsection, this corresponds to having different $E(i)$ which cannot be determined a priori. It follows that the missing detection probability associated with such received signals is higher compared to the ideal case analyzed here. The simplified Detection Probability in the case of real UWB signals depends on energies $E(i)$ collected during Energy computation. It is possible to modify expression 15 for taking into account the terms $E(i)$ of an UWB signal,

$$P_d = \frac{1}{2^{PG}} erfc^{PG} \left(\frac{-E(i)}{\sqrt{2}\sigma_N}\right) \cdot \qquad (16)$$
$$\cdot \prod_{i \neq m} \left(1 - \frac{1}{2^{PG}} erfc^{PG} \left(\frac{-E(m)}{\sqrt{2}\sigma_N}\right)\right).$$

Generally it is not possible to determine whether the detection probability is larger or smaller than in case of $p(t) = \delta(t)$ because it depends on energies $E(m)$. Moreover, the definition of lock-point implies that the energy step $E(i)$ corresponds to the position of the maximum energy, which generally is not proven for UWB channels due to their statistical nature. In addition, if the PRI is short Inter-Symbol-Interference affects the energy steps $E(m)$ and thus modifies P_d. While in presence of $\delta(t)$ the herein proposed scheme can be employed for obtaining high synchronization accuracies (on the order of 1 ns), the nature of UWB signals makes it unsuitable for detecting first paths of received UWB signals. In fact, as will be shown in the next section, the maximum detection algorithm leads to higher synchronization performance in presence of real UWB pulses.

To obtain better synchronization accuracies, one of the possible solutions consists of employing a searchback algorithm [5]. The collection of Energies in ADE can be thus processed by starting from the corresponding index i which identifies $max\{ADE\}$ and then searching back by comparing the values of ADE in adjacent indexes. These algorithms are based on three parameters: The false alarm probability, the number of adjacent noise samples and the searchback window length [5] that have to be set according to the channel characteristics.
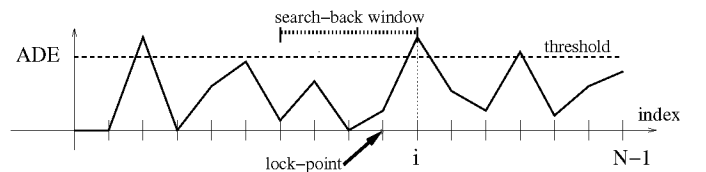

Fig. 5. Searchback algorithm

A searchback algorithm scheme is given in figure 5. In this work, the algorithm is applied starting from the maximum energy computed in ADE and then searches back with an

appropriate window whose length is set a priori. It continues until all the samples within the window bounds are all under the threshold. When this condition holds, the position of lock point is stored. If the search rolls back to the first values in ADE, the window is decreased accordingly until it reaches width of 1 sample and the position of lock point will be stored as 0. Searchback algorithms proposed in [5] are based on finer resolutions (the integration duration is ideally 1 ns) and on non–overlapping integration windows while here the synchronization accuracies are higher and integration windows are superposed. Notwithstanding this, due to the multipath the energy steps computed during the first phase of this synchronization algorithm present similar properties to data collected by using non–overlapping integration windows. The use of these algorithms is worthy of consideration because they help tackle spurious peaks in ADE caused by noise.

III. SIMULATIONS

A first model verification has been obtained through Matlab simulations aimed at calculating the Detection Probability. Figure 6 shows the comparison between the analytical model of equation 14 and simulations obtained for different processing gains with a sampled Dirac Delta: The operating conditions are $T_w = 80ns$, $T_s = 200ns$ and $t_{step} = 5ns$. The model matches the simulations results.
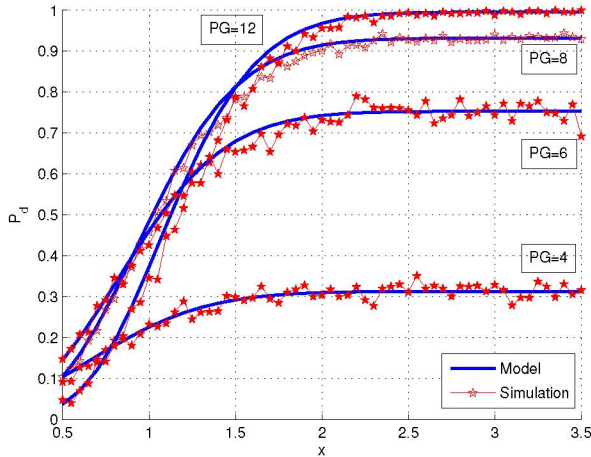

Fig. 6.   Comparison between P_d model and simulation

For $PG = 8$ the detection probability does not reach 1. This is due to the term $\left(1 - \frac{1}{2^{PG}}\right)^{N-2}$ which, given PG, decreases as N increases. At higher PG, i.e. 12, the curves reach quickly the maximum probability as x increases because the second term in brackets tends to zero.

The algorithm performance has been tested with Mean–Absolute–Error (MAE) simulations in which the synchro–nization process has been averaged on 100 realizations. At each iteration, the waveform realization has been uniformly randomized. In the case of the Dirac delta, the simulation consisted only of repeating the algorithm 100 times. The algorithm has been tested with different synchronization steps, in particular $t_{step} = 10ns$ and $t_{step} = 5ns$. For real UWB

pulses two cases are considered: In the first a maximum detection algorithm as in equation 13 has been employed. In the second a searchback algorithm has been used. For the second case simulations, the search–back window length is 3 for $t_{step} = 10ns$ and 6 for $t_{step} = 5ns$, and the threshold has been set to $max\{ADE\} - 1$ in all cases. Even though the definition of False Alarm Probability differs from [5] this choice implies automatically that a missing detection probability is set. For the sampled Dirac delta pulses, only the maximum detection algorithm has been simulated.

In all simulations the equivalent noise bandwidth is 10 GHz and a delay uniformly distributed in $[0, PRI]$ has been in-cluded in all simulations. The UWB pulses are obtained through the 802.15.4a Line-Of-Sight (LOS) channel model CM1 and CM3 (Residential and Office Line–of–Sight) [6] and the Matlab simulation environment combine the pulses in order to take into account the Inter–Symbol–Interference of the preamble sequence. The integration time T_w is $30ns$ in all cases as specified in [7]. The synchronization error has been computed as $min\{|\tau - t_{synch}|, |T_s + \tau - t_{synch}|\}$.
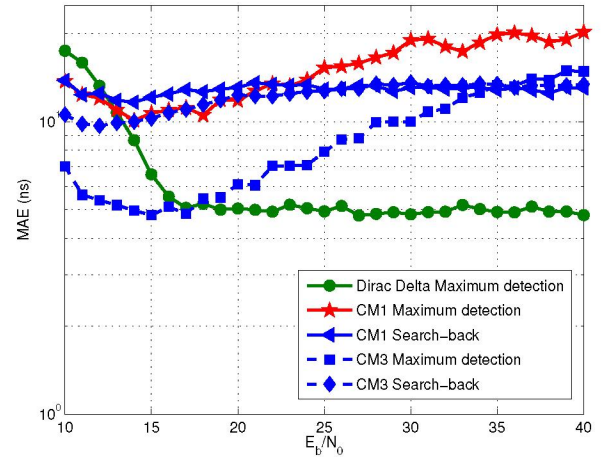

Fig. 7.   Mean–Absolute–Error for CM1, CM3 and Dirac Delta, with $T_w = 30ns$, $t_{step} = 10ns$, $T_s = 100ns$

For taking into account Inter–Symbol–Interference. The sim–ulations are organised in two groups: A repetition period of $T_s = 100ns$ and of $T_s = 60ns$ are chosen for the first and the second group, respectively. Figures 7 and 8 show the synchronization Mean–Absolute–Errors for $T_s = 100ns$ with different synchronization accuracies, $t_{step} = 5ns$ and $t_{step} = 10ns$, respectively. For a Dirac Delta the MAE converges and does not increase at high SNR. This is due to the expression of P_d: As shown in figure 6 the Detection Probability tends to a constant value and, considering that MAE is proportional to P_d, it presents an asymptotic trend. On the other hand, for the UWB pulses we notice an MER increase for high SNR. This is due mainly to the signal shape. In presence of UWB signals, supposing infinite SNR, vector ADE includes multiple incremental values because the channel sputters the signal energy and forms local groups of multipaths. It follows that it is possible to detect multiple rising energy steps $E(i)$.
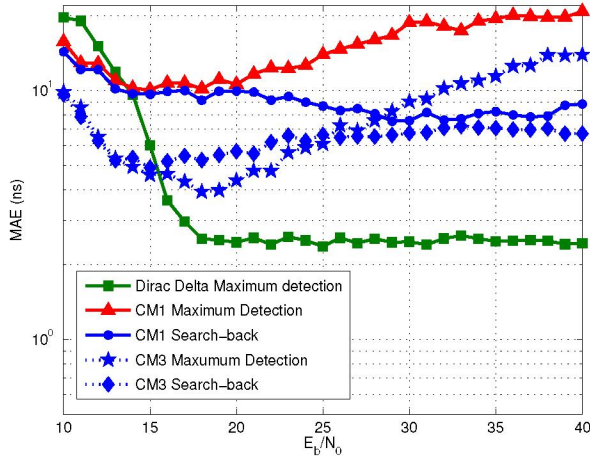
In the case of $t_{synch} = 10ns$, the UWB signal ener–

Fig. 8. Mean–Absolute–Error for CM1, CM3 and Dirac Delta, with $T_w = 30ns$, $t_{step} = 5ns$, $T_s = 100ns$

Fig. 9. Mean–Absolute–Error for CM1, CM3 and Dirac Delta, with $T_w = 30ns$, $t_{step} = 10ns$, $T_s = 60ns$

gies are "sliced" coarsely: For both the CM1 and CM3 the searchback algorithm leads to about the same performance because energies $E(i)$ in vector ADE do not differ from each other. On the other hand, for the maximum detection algorithm the results are quite different because the maximum energy variations of CM1 are different from CM3. While for CM1, the maximum $E(i)$ is quite far from the first path arrival time, for CM3 it is shown that the maximum $E(i)$ is near the first-path arrival time. At high SNR the accuracies decrease because multiple maximums are detected in vector ADE. In the case of $t_{synch} = 5ns$ the effects summarized above are deemphasized because energies are sliced finely. The search-back algorithm gives better results because the obtained ADE better approximates the energies obtained with the typical resolution employed for TOA estimation. In summary, the synchronization accuracies are better for CM3 because energies $E(i)$ are distributed in a favourable condition for the algorithm.

Figures 9 show the synchronization MAE for $T_s = 60ns$ in the case synchronization accuracy is 10 ns. Results show that ISI affect synchronization accuracy for the search-back algorithm case because the energies of the multipath groups are significantly modified by ISI. The curves are smoother but for CM1, results are worse with respect to the case of $T_s = 100ns$ of figure 7.

Generally the search-back algorithm helps tackle the problem of computing multiple peaks in vector ADE at high SNR. In summary, the obtained synchronization accuracies are limited for signal to noise ratios smaller than 40 dB. Even though it does not allow high accuracies, results show that the synchronization algorithm represents a low-complexity solution for Energy Detection receivers with reduced complexity.

The main drawback of this scheme is related to the long time required for computing energies. With i.e. $PG = 10$, $T_s = 100ns$, $t_{step} = 5ns$, $T_w = 30ns$ the algorithm locks in 40μ s. This poor synchronization time is unavoidable because the receiver employs a 1-bit converter only.
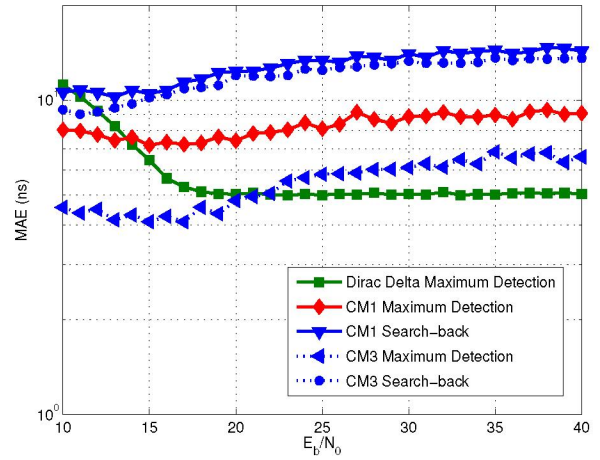
IV. CONCLUSIONS

This paper has investigated the possibility to perform coarse synchronization in a simplified Energy Detection receiver employing a "Differential Energy Detector". Through a first mathematical discussion, the synchronization algorithm has been defined and its operation in the case of an ideal Dirac Delta signal and in the case of realistic UWB pulses has been presented. Preliminary discussions and results obtained by Matlab simulations show that is possible to perform synchronization both for the two kinds of pulses provided that for the UWB waveforms energies are computed with a search-back algorithm. Due to the extremely low-complexity of the receiver, that is the 1-bit-only information available for calculations, the drawback of this scheme is the long synchronization time required for capturing pulse energies.

REFERENCES

[1] P. Chelong et al., "Synchronization, toa and position estimation for low–complexity ldr uwb devices," in In Proc. Int. Conf on UWB, Sept. 2005.
[2] M. Crepaldi et al., "Energy detection uwb receiver design using a multiresolution vhdl-ams description," in In Proc. SIPS 2005, Athens, Greece, Nov. 2005.
[3] ——, "Uwb receiver design and two–way–ranging simulation using vhdl–ams," in In Proc. PRIME 2006, Otranto, Italy, June 2006.
[4] L. Stoica et al., "An ultrawideband system architecture for tag-based wireless sensor networks," IEEE Trans. Veh. Technol., vol. 54, no. 5, pp. 1632–1645, 2005.
[5] I. Guvenc et al., "Non-coherent toa estimation in ir-uwb systems with different signal waveforms," in In IEEE International Conference on Broadband Networks, vol. 2, Oct. 2005, pp. 539–550.
[6] IEEE 802.15 wpan low rate alternative phy task group 4a (tg4a). [Online]. Available: http://www.ieee802.org/15/pub/TG4a.html
[7] I. Guvenc et al., "Toa estimation for ir-uwb systems with different transceiver types," IEEE Trans. Microwave Theory Tech., vol. 54, no. 4, pp. 1876–1886, 2006.